Published by Institute of Physics Publishing for SISSA/ISAS
Received: February 15, 2002
Accepted: April 2, 2002

Investigating the supersymmetric explanation of anomalous CDF lepton(s) photon(s) missing-E_T events

Benjamin C. Allanach, Smaragda Lola and K. Sridhar*

CERN
Geneva 23, CH-1211, Switzerland
E-mail: allanach@cern.ch, magda.lola@cern.ch, krishnamoorthy.sridhar@cern.ch

Abstract: The recent excess over the Standard Model prediction in the $\mu\gamma$ missing-E_T ($\not\!\!E_T$) channel reported by CDF can be well-explained by resonant smuon production with a single dominant R-parity violating coupling λ'_{211}, in the context of models where the gravitino is the lightest supersymmetric particle. The slepton decays to the lightest neutralino and a muon followed by neutralino decaying to a gravitino and photon. The kinematical distributions are fitted well by our hypothesis and we use them to constrain the available parameter space. The model also provides an explanation for the $ee\gamma\gamma\not\!\!E_T$ event observed in Run I of the Tevatron by the CDF experiment. Our model predicts an excess of between 5 and 35 events in a $\gamma\not\!\!E_T$ channel at Run I. We provide predictions for signatures expected by the model at Run II.

Keywords: Beyond Standard Model, Supersymmetric Standard Model, Hadronic Colliders.

*On leave of absence from the Tata Institute of Fundamental Research, Homi Bhabha Road, Mumbai 400 005, India.

Contents

1. Introduction

In spite of the remarkable agreement of the Standard Model (SM) with available data from high-energy experiments, it is expected to be only a low-energy manifestation of a more complete theory at energy scales beyond a TeV. This new TeV-scale physics is expected to ameliorate the problems that beset the SM because of the huge discrepancy between the electroweak scale and the Planck (or GUT) scale. The most popular candidate for such an extension of the SM has been its supersymmetric generalisation which, in its simplest form, is the Minimal Supersymmetric Standard Model (MSSM). The gauge structure of the MSSM essentially replicates that of the SM but, in the Yukawa sector, in addition to the usual Yukawa couplings of the fermions to the Higgs (responsible for the fermion masses), other interactions involving squarks or sleptons are possible.

The relevant part of the superpotential containing the Yukawa interactions involving squarks or sleptons is given in terms of the chiral superfields by

$$W_{RPV} = \frac{1}{2}\lambda_{ijk} L_i L_j \bar{E}_k + \lambda'_{ijk} L_i Q_j \bar{D}_k + \frac{1}{2}\lambda''_{ijk} \bar{U}_i \bar{D}_j \bar{D}_k + \mu_i L_i H_2 \,, \tag{1.1}$$

where L (Q) are the left-handed lepton (quark) superfields while $\bar{E}, \bar{D}$, and $\bar{U}$ contain the corresponding right-handed fields, and i, j, k generation indices. λ and λ' are lepton-number ($L-$) violating, the λ'' couplings are baryon-number ($B-$) violating and the last term is a L-violating bilinear coupling. The simultaneous existence of the $L-$ and $B-$-violating couplings can induce a catastrophically high rate for proton decay and are usually forbidden

JHEP04(2002)002

in the MSSM by invoking a discrete symmetry called R-parity where $R = (-1)^{(3B+L+2S)}$, where S is the spin of the particle, so that the SM particles have $R = 1$, while their superpartners have $R = -1$. However, R-conservation is too strong a requirement to avoid the unwanted proton decay for it can be effectively forbidden assuming that either the L-violating or the B-violating couplings in eq. (1.1) are present, but not both. Limits on the R-violating couplings derived from existing experimental information have been summarised in ref. [1].

In the presence of R-violating couplings, the lightest supersymmetric particle (LSP), which is usually the neutralino, is *not* stable and can decay through R-violating modes [2]. This is in contrast to the R-conserving MSSM where the LSP is stable and this stability is a very desirable feature if the LSP were to be a viable dark matter candidate. In the R-violating case, the neutralino cannot be a dark matter candidate unless the R-violating couplings are very small so as to ensure that the lifetime of the neutralino is much larger than the age of the universe. The situation can be saved, however, in theories where the gravitino (the spin-3/2 superpartner of the graviton) is the lightest supersymmetric particle: a circumstance that can be realised very naturally in theories with gauge-mediated supersymmetry breaking [3]. The light gravitino is long-lived enough to account for dark matter (or, at least, the hot component of dark matter) even in the presence of R-violating couplings [4].

2. Physics of light gravitinos

Even though gravity is naturally incorporated if supersymmetry is realised as a gauge symmetry, the gravitational sector is usually irrelevant for collider phenomenology because of the feebleness of gravitational interactions. But if supersymmetry is broken spontaneously, the gravitino acquires a mass by absorbing the would-be goldstino and in the high-energy limit the gravitino has the same interactions as the goldstino [5]. These interactions are proportional to $1/m_{\tilde{G}}$ and consequently the interactions of the gravitino can become important for processes at collider energies in the $m_{\tilde{G}} \to 0$ limit. The mass of the gravitino is related to F_0, the fundamental scale-squared of supersymmetry breaking, by the following relation:

$$m_{\tilde{G}} = \frac{F_0}{\sqrt{3}M_P} \,. \tag{2.1}$$

$M_P = 2.4 \times 10^{18}$ GeV is the reduced Planck mass, and using this value one obtains

$$m_{\tilde{G}} = 5.9 \times 10^{-5} \frac{F_0}{(500\,\mathrm{GeV})^2}\,\mathrm{eV} \,. \tag{2.2}$$

Given a lower bound on the value of F_0 one can then deduce a lower bound on the mass of the gravitino which, in turn, yields a bound on the interactions of the gravitino with the SM particles.

To make these considerations more concrete, we write down the relevant part of the supersymmetric lagrangian containing the gravitino interactions:

$$\mathcal{L} = \frac{1}{8M_P}\bar{\lambda}^A \gamma^\rho \sigma^{\mu\nu} \tilde{G}_\rho F^A_{\mu\nu} + \frac{1}{\sqrt{2}M_P}\bar{\psi}_L \gamma^\mu \gamma^\nu \tilde{G}_\mu D_\nu \phi + \mathrm{h.c.}\,, \tag{2.3}$$

where $\tilde{G}$ is the gravitino field, λ^A the gaugino field, $F^A_{\mu\nu}$ the corresponding field strength and (ϕ, ψ) the scalar and the fermionic components of the chiral supermultiplets. At the level of a effective interaction, the spin-3/2 gravitino field can be well described by its spin-1/2 goldstino component when it appears as an external state, i.e.

$$\tilde{G}_\mu = \sqrt{\frac{2}{3}} \frac{i}{m_{\tilde{G}}} \partial_\mu \tilde{G} \,. \tag{2.4}$$

Using this limit in eq. (2.3), allows one to compute the decay widths of the process $\chi_i \to \gamma/Z\tilde{G}$, for example. These are:

$$\begin{aligned} \Gamma\left(\chi_i^0 \to \gamma\tilde{G}\right) &= \frac{\kappa_{i\gamma}}{48\pi} \frac{m^5_{\chi_i^0}}{M_P^2 m^2_{\tilde{G}}} \\ \Gamma\left(\chi_i^0 \to Z\tilde{G}\right) &= \frac{2\kappa_{iZ_T} + \kappa_{iZ_L}}{96\pi} \frac{m^5_{\chi_i^0}}{M_P^2 m^2_{\tilde{G}}} \left[1 - \frac{m_Z^2}{m^2_{\chi_i^0}}\right]^4 , \end{aligned} \tag{2.5}$$

where

$$\begin{aligned} \kappa_{i\gamma} &= |N_{i1}\cos\theta_W + N_{i2}\sin\theta_W|^2 \\ \kappa_{iZ_T} &= |N_{i1}\sin\theta_W - N_{i2}\cos\theta_W|^2 \\ \kappa_{iZ_L} &= |N_{i3}\cos\beta - N_{i4}\sin\beta|^2 \,. \end{aligned} \tag{2.6}$$

The N_{ij} are the χ_i^0 components in standard notation. The neutralino can also decay into a gravitino and a neutral Higgs particle and the corresponding expressions for these are

$$\Gamma(\chi_i^0 \to \phi\tilde{G}) = \frac{\kappa_{i\phi}}{96\pi} \frac{m^5_{\chi_i^0}}{M_P^2 m^2_{\tilde{G}}} \left[1 - \frac{m_\phi^2}{m^2_{\chi_i^0}}\right]^4 , \tag{2.7}$$

where the Higgsino components are given by

$$\begin{aligned} \kappa_{ih^0} &= |N_{i3}\sin\alpha - N_{i4}\cos\alpha|^2 \\ \kappa_{iH^0} &= |N_{i3}\cos\alpha + N_{i4}\sin\alpha|^2 \\ \kappa_{iA^0} &= |N_{i3}\sin\beta + N_{i4}\cos\beta|^2 \,. \end{aligned} \tag{2.8}$$

From the above equations, it is easy to convince oneself that the decay modes into the photon dominates over the decays into the Z or the neutral Higgs boson because the decays into the latter states are phase-space suppressed. If the neutralino is bino-dominated, then the branching ratio into a photon and gravitino is nearly 100%.

3. The CDF anomaly

CDF has recently presented results on the production of combinations involving at least one photon and one lepton (e or μ) in $p\bar{p}$ collisions at $\sqrt{s} = 1.8\,\mathrm{TeV}$, using $86.34\,\mathrm{pb}^{-1}$ of Tevatron 1994-95 data [6]. In general the results were consistent with the standard model, however 16 photon-lepton events with large $\not{E}_T$ were observed, with 7.6 ± 0.7 expected. Moreover, 11 of these events involved muons (with 4.2 ± 0.5 expected) and only 5 electrons (with 3.4 ± 0.3 expected), therefore there is a clear asymmetry, which indicates the existence of a lepton flavour-violating process involving muons.

As we proposed in an earlier paper [7], we suggest that the excess can be simply understood in terms of smuon resonance production via an L-violating λ' coupling[1] which decays predominantly into a bino-dominated neutralino and a muon, with the neutralino further decaying into a photon and a gravitino. The production and decay has been shown in the Feynman diagram in figure 1. The merit of this model that we proposed is that it is a natural explanation of the characteristics of the CDF anomaly: 1) the flavour-dependence is a direct consequence of the R-violating coupling and, 2) the fact that the excess is seen in final states involving photons emerges very neatly in the model because the decay $\chi_1^0 \to \gamma\tilde{G}$ dominates overwhelmingly over other decay modes. We note that both R-parity violation and the existence of a very light gravitino are needed to explain the anomaly, in our model. Nonetheless, we emphasise that if one has R-parity violating supersymmetry, a light gravitino is preferable from dark matter considerations, as explained in the previous section.

A light gravitino has also been previously invoked [9] to explain the $ee\gamma\gamma\not{E}_T$ CDF event [11], detected in searches for anomalous production of missing transverse energy ($\not{E}_T > 12\,\mathrm{GeV}$), in events containing two isolated, central photons. The event was explained in terms of the R-conserving production of a pair of selectrons and the subsequent decay of each of these selectron into a $\gamma\tilde{G}$ final state. It has been shown [10] that this explanation is excluded in the framework of the minimal gauge mediated supersymmetry breaking (GMSB) model, because of the anomalously large rates for jets $+\gamma + \not{E}_T$ events predicted by this model. The problem can be traced back to the mass spectrum of the minimal models: in this version of GMSB models the charginos and second-lightest neutralinos are light which lead to large jets $+\gamma + \not{E}_T$ rates not seen in experiment. However, in non-minimal models of GMSB the charginos and the second-lightest neutralinos are heavier and one can have a viable explanation of the CDF event in these models which is not in conflict with other existing experimental information. For our purposes, again a light neutralino of 100 GeV Mass and a reasonably light smuon in the mass range of about 150 GeV is needed but we require all the other supersymmetric particles to be very massive. In the present paper, we perform detailed fits to the experimentally measured distributions of the anomalous events in order to determine the masses of the lightest neutralino and the smuon with the assumption that all the other masses are heavy enough not to be produced at the Tevatron. We do not attempt to place our scenario in the context of some specific model of GMSB, but point out that this is indeed possible in the case of non-minimal models of GMSB. A detailed model-dependent study is relegated to a later publication.

4. Constraints

If the anomalous events seen by the CDF experiment are to be attributed to the production of a smuon resonance involving an R-violating operator, we can ask what the precise form of this operator is. To get a substantial cross-section for the production of the smuon resonance one needs to couple it to valence quarks in the initial state. This observation is then

[1] Smuon resonances at hadron colliders have been previously studied in a different context [8].

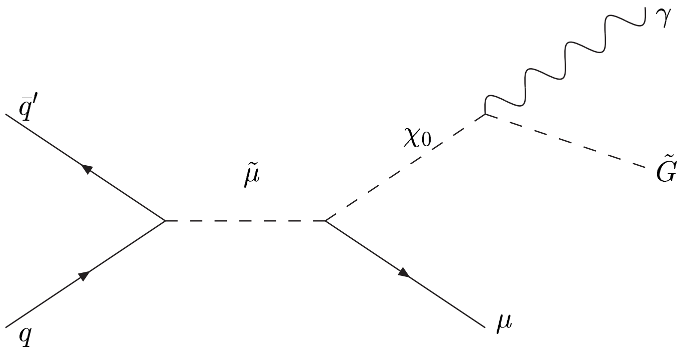

Figure 1: Feynman diagram of resonant smuon production followed by neutralino decay.

JHEP04(2002)002

sufficient to specify the R-violating operator to be $L_2 Q_1 \bar{D}_1$ corresponding to the coupling λ'_{211}. This operator generates the interactions $\tilde{\mu} u \bar{d}$ and $\tilde{\nu}_\mu d \bar{d}$ (and charge conjugates), along with other supersymmetrised copies involving squarks. Therefore, if we invoke this operator to explain the CDF anomaly we will simultaneously predict effects in other channels which will manifest themselves through the production of either sneutrinos or squarks. In our model, since we take the squarks to be heavy, their effects on experimental observables will be negligible. On the other hand, the sneutrinos are necessarily relatively light and can be produced resonantly and should lead to observable effects in experimental situations. In the present paper, we not only analyse the smuon resonance production in the context of the CDF anomaly but also provide predictions for both the smuon and the sneutrino channels at Run I and Run II of the Tevatron. The smuons, sneutrinos and the lightest neutralino are all light enough to be pair-produced through R-conserving channels. We also provide predictions for these cross-sections at Run I and Run II.

For our analysis, we have essentially four parameters at our disposal: the gravitino mass, $m_{\tilde{G}}$, the bino mass parameter M_1, the smuon mass parmeter, $m_{\tilde{\mu}}$ and the R-violating coupling λ'_{211}. The coupling, λ'_{211}, is constrained from $R_\pi = \Gamma(\pi \to e\nu)/(\pi \to \mu\nu)$ [12] to be $< 0.059 \times \frac{m_{\tilde{d}_R}}{100\,\mathrm{GeV}}$ [1]. We note that the constraint involves a squark mass which is large in our model. So the constraint from R_π for our purposes is not very relevant. However, instead of simultaneously fitting the four parameters using the experimental data, we choose to work with fixed values of the λ'_{211} and $m_{\tilde{G}}$ and perform fits in M_1 and $m_{\tilde{\mu}}$. While the production of the smuon resonance is through the R-violating mode, its decay needs to go through the R-conserving channel to a neutralino and muon final state. The R-violating decay of the slepton is possible but constrained, in principle, by the Tevatron di-jet data [13] which exclude a $\sigma.B > 1.3 \times 10^4$ pb at 95% C.L. for a resonance mass of 200 GeV. However, in practice this does not provide a restrictive bound upon our scenario as long as the R-violating coupling is sufficiently small. We also add that the di-jet bound is not very restrictive because it suffers from a huge QCD background. By restricting λ'_{211} to be small, we also avoid the possible R-violating decays of the $\chi_1^0 \to \mu j j$

or $\chi_1^0 \to \nu jj$ final states. With these considerations in mind we choose $\lambda'_{211} = 0.01$. The gravitino mass is also fixed at 10^{-3} eV in our fits. We will discuss the effects of varying the gravitino mass and the R-violating coupling later in this paper.

5. Defining the model

The supersymmetric model parameters that are relevant for our discussion, are: M_1, M_2, μ, $\tan\beta$ and m_0, which determine the chargino, neutralino and sfermion masses at low energies. Since no other exotic cascade decays at CDF, are observed, we assume that:

- Charginos and other superparticles (except the slepton and the lightest neutralino) are too heavy to be produced at the current energies.
- The decays of the lightest neutralino to gauge bosons other than the photon are coupling and/or phase-space suppressed.

These considerations constrain the allowed supersymmetric parameter space, which as we are going to show, still has some generality within it. To see this, let us look at the formulae that give the chargino and neutralino masses and mixings in terms of the fundamental supersymmetric parameters.

The tree-level neutralino mass matrix in the $\psi_j^0(-i\tilde{B}, -i\tilde{W}_3, \tilde{H}_1^0, \tilde{H}_2^0)$ basis are the mass eigenstates of the matrix

$$Y = \begin{pmatrix} M_1 & 0 & -m_Z \sin\theta_W \cos\beta & m_Z \sin\theta_W \sin\beta \\ 0 & M_2 & m_Z \sin\theta_W \cos\beta & -m_Z \cos\theta_W \sin\beta \\ -m_Z \sin\theta_W \cos\beta & m_Z \cos\theta_W \cos\beta & 0 & -\mu \\ m_Z \sin\theta_W \sin\beta & -m_Z \cos\theta_W \sin\beta & -\mu & 0 \end{pmatrix} \tag{5.1}$$

and are defined by $\chi_i^0 = N^{ij}\psi_j^0$, with N_{ij} being the unitary matrix which diagonalises Y. The respective mixings in the basis $(\tilde{\gamma}, \tilde{Z})$ instead of $(\tilde{B}, \tilde{W}_3)$, are given by $N'_{j1} = N_{j1}\cos\theta_W + N_{j2}\sin\theta_W$, $N'_{j2} = -N_{j1}\sin\theta_W + N_{j2}\cos\theta_W$, $N'_{j3} = N_{j3}$ and $N'_{j4} = N_{j4}$. Finally, the respective chargino mass matrix in the $(\tilde{W}^{\pm}, \tilde{H}^{\pm})$ basis is

$$X = \begin{pmatrix} M_2 & m_W\sqrt{2}\sin\beta \\ m_W\sqrt{2}\cos\beta & \mu \end{pmatrix}. \tag{5.2}$$

In our work we will not make use of the GUT inspired relation $M_1 = \frac{5}{3}\tan^2\theta_W M_2$, but will instead keep M_1 and M_2 generic. As we see from the above formulae, a light neutralino can arise either via a light M_1, a light M_2, or a light μ. In the second and third cases however, the chargino is also going to be light enough to be seen in cascade decays, which is not the case in CDF data. Moreover, constraining the relative masses of M_1 and M_2 roughly determines the photino component of the lightest neutralino. Under these conditions $\tan\beta$ is expected to play a relatively moderate role. Table 1 contains the lightest chargino and neutralino masses, and the magnitude of the photino-component of the lightest neutralino, for different model parameters. In this section only, we constrain ourselves to small and intermediate values of M_2 and μ, since for larger values our requirements are more easily fulfilled.

		$M_1 = 90\,\mathrm{GeV},\ \tan\beta = 4$				$M_1 = 120\,\mathrm{GeV},\ \tan\beta = 4$			
M_2	μ	$m_{\tilde{\chi}_1^0}$	$m_{\tilde{\chi}_2^0}$	$m_{\tilde{\chi}_1^\pm}$	$\|N_{11}\|$	$m_{\tilde{\chi}_1^0}$	$m_{\tilde{\chi}_2^0}$	$m_{\tilde{\chi}_1^\pm}$	$\|N_{11}\|$
200.	-600.	91.	202.	202.	0.88	121.	202.	202.	0.88
200.	-200.	90.	167.	170.	0.85	118.	168.	170.	0.81
200.	200.	77.	144.	135.	0.71	99.	151.	135.	0.56
200.	600.	88.	191.	191.	0.86	118.	191.	191.	0.85
400.	-600.	91.	396.	397.	0.88	121.	396.	397.	0.88
400.	-200.	90.	197.	200.	0.85	118.	198.	200.	0.83
400.	200.	79.	191.	181.	0.80	104.	196.	181.	0.75
400.	600.	88.	381.	380.	0.87	118.	381.	380.	0.87
600.	-600.	91.	561.	563.	0.88	121.	561.	563.	0.88
600.	-200.	90.	200.	202.	0.85	118.	202.	202.	0.84
600.	200.	79.	201.	191.	0.81	105.	204.	191.	0.78
600.	600.	88.	534.	533.	0.87	118.	534.	533.	0.87
		$M_1 = 120\,\mathrm{GeV},\ \tan\beta = 50$							
200.	-600.	119.	197.	197.	0.87				
200.	-200.	110.	158.	153.	0.96				
200.	200.	109.	156.	150.	0.67				
200.	600.	119.	196.	196.	0.86				
400.	-600.	119.	389.	389.	0.87				
400.	-200.	112.	197.	191.	0.79				
400.	200.	111.	197.	190.	0.78				
400.	600.	119.	388.	388.	0.87				
600.	-600.	119.	547.	547.	0.87				
600.	-200.	112.	203.	197.	0.81				
600.	200.	111.	204.	196.	0.80				
600.	600.	119.	545.	545.	0.87				

Table 1: Light weak gaugino masses and photino component of the lightest neutralino $|N_{11}|$ for various values of $\tan\beta$, M_1, μ.

We see that demanding a lightest neutralino in the range $90 - 120\,\mathrm{GeV}$, with the chargino remaining relatively heavy leads to a neutralino mixing in a photino component that is significantly constrained, and lies in the range (0.81-0.88). This also holds for larger values of M_2, μ which are not included in the table.

We use a single slepton mass parameter $m_{\tilde{l}} \equiv m_{\tilde{\mu},\tilde{e}_R} = m_{\tilde{e},\tilde{\mu}_L}$. Neglecting small fermion mass terms, the tree-level slepton masses are then (for the first two generations)

$$\begin{aligned} m_{\tilde{e},\tilde{\mu}_L} &= m_{\tilde{l}}^2 + \left(\frac{1}{2} - \sin\theta_W^2\right) M_Z^2 \cos(2\beta) \\ m_{\tilde{e},\tilde{\mu}_R} &= m_{\tilde{l}}^2 - \sin\theta_W^2 M_Z^2 \cos(2\beta)\,, \\ m_{\tilde{\nu}_e,\tilde{\nu}_\mu} &= m_{\tilde{l}}^2 + \frac{1}{2}\sin\theta_W^2 M_Z^2 \cos(2\beta) \end{aligned} \tag{5.3}$$

with negligible mixing proportional to the electron and muon masses respectively.

We use the ISASUSY part of the ISAJET7.58 package [14] to generate the spectrum, branching ratios and decays of the sparticles. For an example of parameters, we choose (in the notation used by ref. [14]) $\lambda'_{211} = 0.01$, $m_{3/2} = 10^{-3}\,\text{eV}$, $\tan\beta = 10$, $A_{t,\tau,b} = 0$, μ together with other flavour diagonal soft supersymmetry breaking parameters are set to 2000 GeV. We emphasise that this is a representative point in the supersymmetric parameter space and not a special choice. Any superparticles except the first two generation sleptons, the lightest neutralino and the gravitino do not appear in this analysis because they are too heavy to be produced or to contribute to cascade decays in CDF data.

6. Fitting kinematical distributions

We now simulate the signal events for the process in figure 1. The Standard Model background is taken from ref. [6]. We use HERWIG6.3 [15] including parton showering (but not including isolation cuts) to calculate cross-sections for single slepton production. The slepton mass parameter $m_{\tilde{l}}$ and the bino mass parameter[2] M_1 are allowed to vary in order to see what range of neutralino and slepton masses are preferred by the experiment.

We simulate the detector by the following:

- Photons can be detected if they do *not* have rapidity $1.0 < |\eta| < 1.1$, $|\eta| < 0.05$. The region $0.77 < \eta < 1.0, 75^\circ < \phi < 90^\circ$ is also excluded because it is not instrumented. If these constraints are satisfied, we assume 81% detection efficiency for the photons.
- Muons have a 60% detection efficiency if $|\eta_\mu| < 0.6$ or 45% if $0.6 \leq \eta_\mu \leq 1.1$

Rapidity of a particle is defined as $\eta = -\ln\tan(\theta/2)$, where θ is the longitudinal angle between the particle's momentum and the beam. ϕ is the transverse angle between the particle's momentum and the x-axis. We also implement the cuts used in the experimental analysis to beat the background down: $E_T(\mu) > 25, \text{GeV}$, $E_T(\gamma) > 25\,\text{GeV}$ and $\not{E}_T > 25\,\text{GeV}$. Because we do not perform jet reconstruction, we do not perform isolation cuts.

CDF gave one-dimensional projections in the $\mu\gamma\not{E}_T$ events for the following kinematic variables

$$\begin{aligned}
E_T &= \sqrt{p_x^2 + p_y^2}\,, \\
m_{12} &= \sqrt{p_1 \cdot p_2} \\
M_T^2 &= E_T^2 - p_x^2 - p_y^2 \\
\Delta\phi_{12} &= \phi_1 - \phi_2 \\
H_T &= \not{E}_T + E_T(\gamma) + E_T(\mu) \\
\Delta R_{\mu\gamma} &= \sqrt{\Delta\phi_{\mu\gamma}^2 + (\eta_\mu - \eta_\gamma)^2}\,,
\end{aligned} \tag{6.1}$$

where $p_{x,y}$ are the x and y (i.e. transverse) components of the momentum respectively and $p_{1,2}$ refer to 4-momenta of particles labeled by 1 and 2.

Once we have a statistically large sample of signal events simulated, we have a prediction for the number of expected signal plus background events in bin i of a distribution:

[2]All parameters take their quoted values at the electroweak scale.

N^i_{S+B}. We use the average background presented in ref. [6]. The Poisson distributed probability density function (PDF) of observing N^i_{obs} events compared to N^i_{S+B} is

$$p^i_{S+B}(N^i_{obs}, N^i_{S+B}) = \frac{e^{-N^i_{S+B}} \left(N^i_{S+B}\right)^{N^i_{obs}}}{r} \,. \tag{6.2}$$

In any one distribution, $p_{S+B} \equiv \Pi_i p^i_{S+B}$ gives the total PDF for that distribution, assuming each bin is uncorrelated to the others. Unfortunately, we are not able to make this assumption between different distributions of variables, because they contain data on the same events and should contain some level of correlation. Finally, the log likelihood of signal plus background $\ln p_{S+B}$ is calculated and normalised by subtracting the analogous log likelihood for the Standard Model background prediction

$$-2 \ln L \equiv -2(\ln p_{S+B} - \ln p_B) \,. \tag{6.3}$$

A negative value then indicates that the data favour the signal plus background hypothesis over just background. When performing parameter (x_i) estimation, one determines the equivalent number of σ away from the best-fit point (which has parameters x_b) by

$$(\Delta\sigma)^2 = -2 \left(\ln L(x_i) - \ln L(x_b)\right) . \tag{6.4}$$

The value of $\ln L(x_i)$ calculated is then equivalent to a probability which matches the number of $\Delta\sigma$ that our model fits the data better than the Standard Model in conventional gaussian statistics. Thus, the measure of number of $\Delta\sigma$ here is purely a measure of probability in tails of PDFs, not a statement about the gaussian nature of that PDF.

We now perform a fit to M_1 and $m_{\tilde{l}}$ keeping all other fundamental parameters (but not branching ratios) constant. We must perform the fit one time for each different distribution; because the distributions come from the same events, they are all correlated to some extent. We cannot therefore assume that the distributions are uncorrelated in order to fit more than one distribution at a time, i.e. the correlations must be taken into account. While we can generate the correlations in the signal events by Monte-Carlo, we do not own multi-dimensional data on the kinematic variables in the data. We therefore cannot perform a fit to more than one distribution at any time. However, it is possible to see to what extent the individual fits to each variable are compatible with each other. The fit corresponds to maximising the log likelihood obtained from eq. (6.3) for one of the distributions. In table 2 we present the best fit points, indicating that light neutralino masses, in the range of $67 - 111$ GeV are to be expected. For small M_1 the lightest neutralino mass is determined by M_1, while M_2 controls the chargino mass. If M_2 is heavy (as assumed here), no cascade decays involving charginos are kinematically favoured.

For the rest of this section, we concentrate on the best-fit point for $E_T(\mu)$, because this gives the best likelihood out of all the fits. In table 3, we show the percentage of events making it through each of the cuts for this best-fit point. The table shows that 11.4% of sleptons produced end up as detected $\mu\gamma\not{E}_T$ events in CDF. The cross-section of 0.091 pb predicts a total of 7.86 events in the $\mu\gamma\not{E}_T$ channel. This is higher than the observed excess because the $E_T(\mu)$ distribution itself prefers it.

Variable	M_1 (GeV)	$m_{\tilde{\ell}} - M_1$ (GeV)	$-2\Delta\ln(L)$	$\Delta\sigma$
$E_T(\mu)$	87	35	-10.94	3.31
$E_T(\gamma)$	67	30	-9.36	3.06
$\not{E}_T$	104	47	-6.09	2.47
$m_{\mu\gamma}$	82	23	-9.94	3.15
$M_T(\not{E}_T\mu)$	96	44	-6.54	2.56
$M_T(\not{E}_T\gamma)$	99	24	-8.81	2.97
$M_T(\not{E}_T\gamma\mu)$	84	28	-6.30	2.51
$\Delta\phi_{\not{E}_T\gamma}$	111	33	-5.28	2.30
$\Delta\phi_{\mu\gamma}$	97	26	-8.87	2.98
$\Delta\phi_{\not{E}_T\mu}$	99	25	-9.01	3.00
H_T	72	33	-5.18	2.28
$\Delta R_{\mu\gamma}$	83	24	-6.26	2.50

Table 2: Separate best fit points for each kinematic variable. We display the bino mass parameter M_1, the mass splitting between M_1 and the slepton mass parameter $m_{\tilde{l}}$. We display the difference in log likelihood between our model and the Standard Model $-2\Delta\ln(L)$ and the corresponding number of sigma $\Delta\sigma$ that the model fits the kinematic distribution better than the Standard Model.

The relevant branching ratios of the smuon for this point are

$$\begin{aligned} BR(\tilde{\mu}_L \to \chi_1^0\mu) &= 0.984\,, \\ BR(\tilde{\mu}_L \to \bar{u}d) &= 0.015\,, \\ BR(\tilde{\mu}_L \to \tilde{\mu}\tilde{G}) &= 0.001\,, \end{aligned} \tag{6.5}$$

with a lifetime of 1×10^{-23} sec, whereas for the lightest neutralino we have

$$\begin{aligned} BR(\chi_1^0 \to \tilde{G}\gamma) &= 0.975\,, \\ BR(\chi_1^0 \to \tilde{G}e^-e^+) &= 0.019\,, \end{aligned} \tag{6.6}$$

with a lifetime of 1×10^{-19} sec. At such small values of λ'_{211} and $m_{\tilde{G}}$, R-parity violating decays of the lightest neutralino are negligible. The light sparticle masses are

cut	percentage
detected μ	52.1
$\not{E}_T > 25\,\mathrm{GeV}$	41.7
detected $E_T(\gamma) > 25\,\mathrm{GeV}$	20.8
detected $E_T(\mu) > 25\,\mathrm{GeV}$	11.4
σ	0.091 pb

Table 3: Percentage of SUSY events that satisfy cumulative cuts for $\mu\gamma\not{E}_T$ events at CDF, Run I for the best-fit point. Events that pass a cut on a given row also pass those cuts on rows above. The γ-in-active-region cut is described in the text. The cross-section after all cuts is displayed on the last row.

$$m_{\chi_1^0} = 86.8\,\mathrm{GeV}\,, \quad m_{\tilde{e}_L,\tilde{\mu}_L} = 130.8\,\mathrm{GeV}\,, \quad m_{\tilde{\nu}_L} = 104.2\,\mathrm{GeV}\,, \quad m_{\tilde{e}_R,\tilde{\mu}_R} = 129.7\,\mathrm{GeV}\,, \tag{6.7}$$

whereas we have set all of the other sparticles except for the gravitino to be heavy (around 2000 GeV), so that they play no role in our analysis.

For this best-fit parameter point, we show the predicted distributions of lepton E_T, photon E_T and $\not{E}_T$ in the histograms of figure 2 and compare them with the excess of the data over the Standard Model background. $\Delta\sigma$ is labeled on each plot and is the

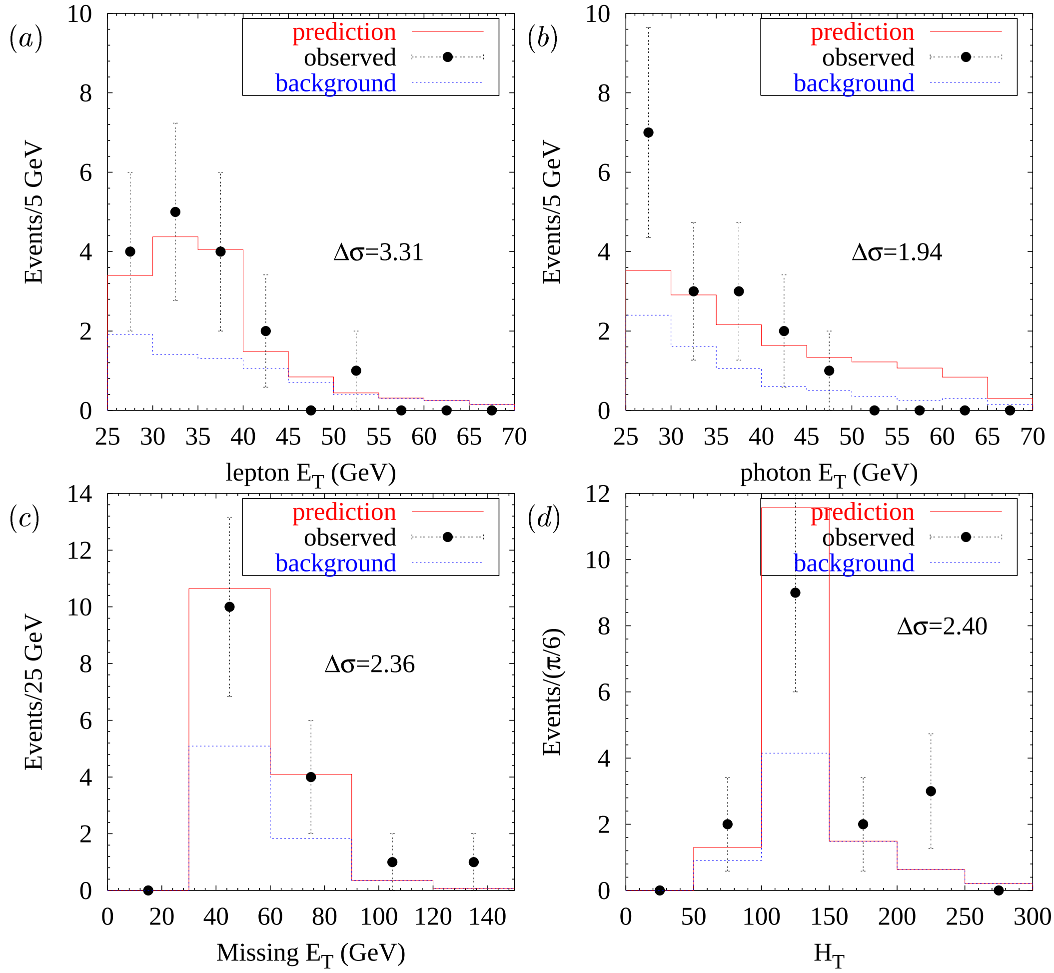

Figure 2: Energy distributions for the $\mu\gamma\not{E}_T$ events. We show the distributions in (a) lepton E_T, (b) photon E_T, (c) $\not{E}_T$ and (d) H_T. The solid red histogram is signal plus background for our best-fit point, the blue dashed histogram is the Standard Model background and the black points (with $\sqrt{N}$ error-bars imposed) are the observed number of events.

equivalent number of sigma that this best-fit point fits a particular distribution better than the Standard Model. Obviously the largest $\Delta\sigma = 3.31$ is for the lepton E_T, since the fit is performed to this variable. But we also see that at this point, the other distributions also fit the data better than the Standard Model: all fit the data better than the Standard model to, at least, 2σ except for the fits to $E_T(\gamma)$ for which $\Delta\sigma = 1.94$. The photon E_T seems to be steeper in the data than in either the Standard Model or in our model and this is a feature at other values of $M_1, m_{\tilde{l}}$. In figure 3 we show the mass distributions. The data seems to indicate a bump extra to the Standard Model at lower values of $m_{\mu\gamma}$, as shown in figure 3a. The angular distributions in figure 4 show that our best-fit point fits the observed excess well in events where the γ and $\not{E}_T$ are roughly back-to-back in figure 4a. While figure 4b does not seem a particularly better fit than the Standard Model by eye, nearly all of the difference in $\ln L$ comes from the last bin, where the Standard Model predicted hardly any events.

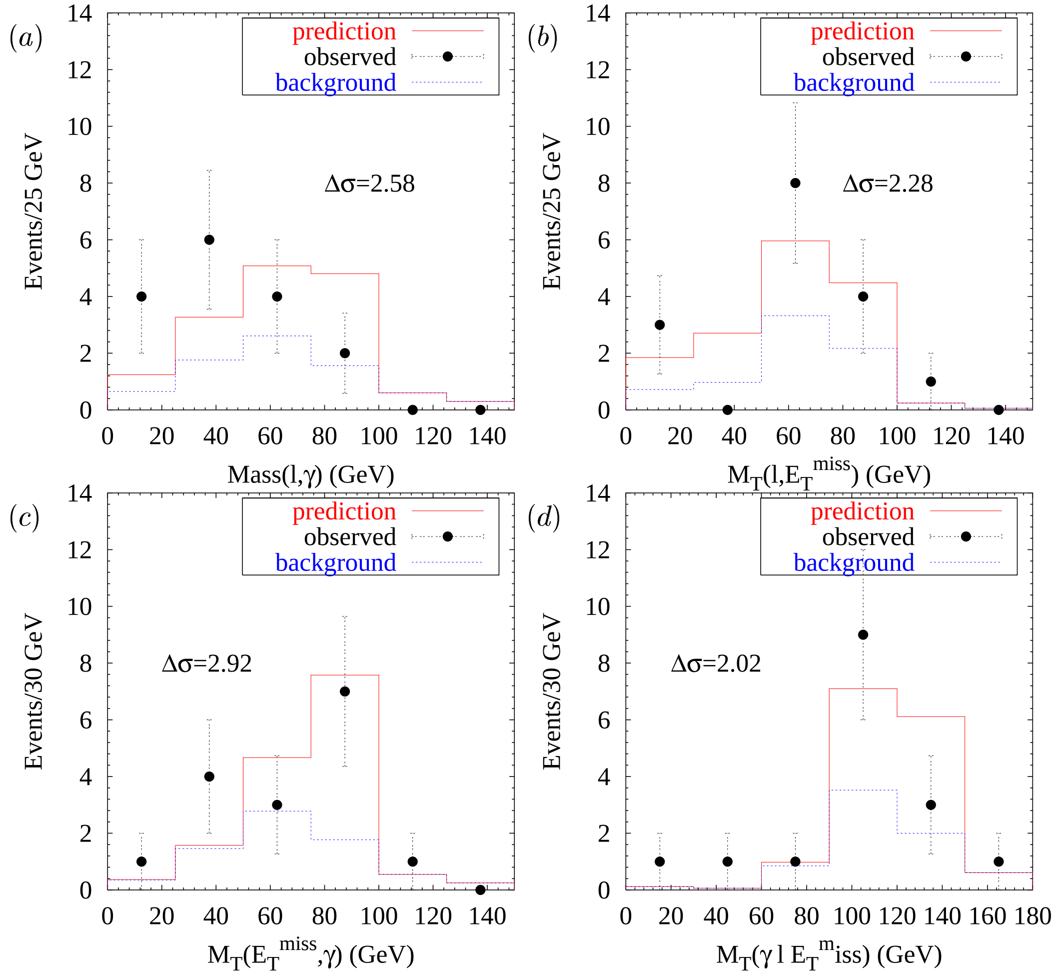

Figure 3: Mass distributions for the $\mu\gamma\not{E}_T$ events. We show the distributions in (a) the invariant mass of the μ-γ pair, (b) transverse mass of $\mu\not{E}_T$, (c) transverse mass of $\gamma-\not{E}_T$ and (d) transverse mass of the $\gamma-\not{E}_T-\mu$ subsystem. The solid red histogram is signal plus background for our best-fit point, the blue dashed histogram is the Standard Model background and the black points (with $\sqrt{N}$ errorbars imposed) are the observed number of events.

To calculate 95% $C.L.$ regions, we scan over the parameters $\Delta m \equiv m_{\tilde{l}} - M_1$ and M_1, calculating $(\sigma)^2$ from eq. (6.4) at each point and for each kinematical distribution. The 95%$C.L.$ is then given by $(\sigma)^2 = -2\Delta \ln L_{BF} + 5.99$, where $\ln L_{BF}$ is the log likelihood at the best-fit point of the kinematic variable being examined. The 95% $C.L.$ regions of Δm and M_1 for each separate fitted kinematical distribution are displayed in figure 5. The horizontal region at the bottom of the plot displays the LEP bound from neutralino pair production where the neutralinos decay to photons and $\not{E}_T$ [16]. We note [17] that analysis of LEP2 data at the highest energies should be able to cover the region up to $M_1 = 100\,\mathrm{GeV}$ or so. The "overlap" region $\Delta m \approx 30 - 40\,\mathrm{GeV}$ and $M_1 \approx 90 - 120$ is encouragingly within the 95% confidence-level regions for all distributions except for $E_T(\gamma)$ (shown as the area inside the white line in figure 5a), which prefers $M_1 < 90\,\mathrm{GeV}$, below the LEP bound. Ideally, a correlated fit would be performed to all distributions simultaneously. Then, the significance of not having such a good fit for $E_T(\gamma)$ in the

JHEP04(2002)002

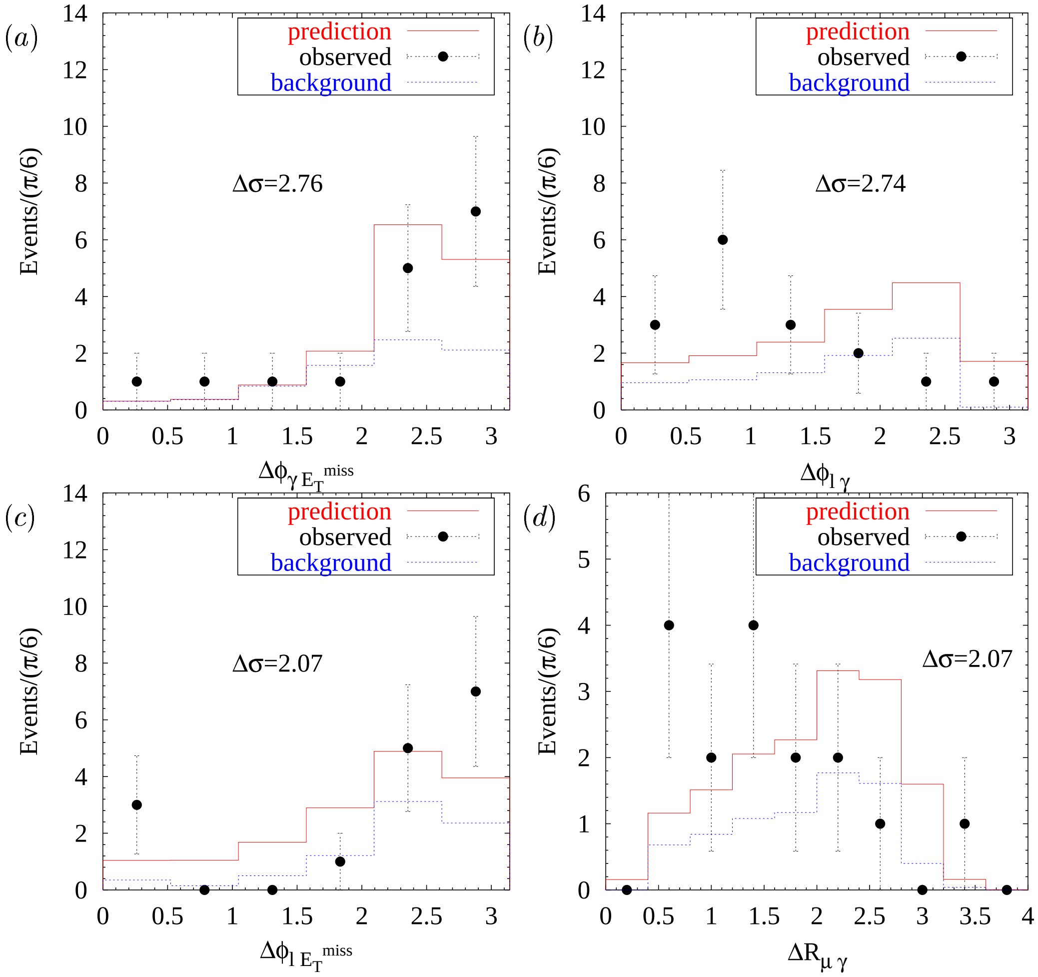

Figure 4: Transverse angular distributions for $\mu\gamma\not{E}_T$ events. We show the distributions in the transverse angle between (a) $\gamma\not{E}_T$, (b) $\mu\gamma$, (c) $\mu\not{E}_T$ and (d) $\Delta R_{\mu\gamma}$. The solid red histogram is signal plus background for our best-fit point, the blue dashed histogram is the Standard Model background and the black points (with $\sqrt{N}$ errorbars imposed) are the observed number of events.

overlap region could be calculated. The most constraining variables are $E_T(\mu)$ and $m_{\mu\gamma}$, which require $(\Delta m, M_1) < (50, 200)$ GeV and $(40, 150)$ GeV respectively. The $M_T(\not{E}_T, \gamma)$ region constrains $M_{\chi_1^0}$ to be less than 120 GeV. The H_T variable is not plotted because it does not constrain any of the parameter space at the 95% C.L.

We now display predictions for various quantities overlaid upon the 95% C.L. region from the $E_T(\mu)$ distribution for different values of M_1 and Δm. For example, in figure 6a, it is shown that the expected number of detected signal $\mu\gamma\not{E}_T$ events (including the cuts described above) is 3-7 in the 95% C.L. region. Each parameter point specifies a particular sneutrino mass by eq. (5.3), and the λ'_{211} coupling will also lead to resonant production of sneutrinos. The sneutrinos decay dominantly into neutrino and neutralino, leading to a $\gamma\not{E}_T$ signal. We use identical cuts to that used for the $\mu\gamma\not{E}_T$ channel, except for the cuts involving muons. figure 6b shows that between 5 and 35 events of this nature are expected within the 95% C.L. region. Standard Model backgrounds should be small, with dominant

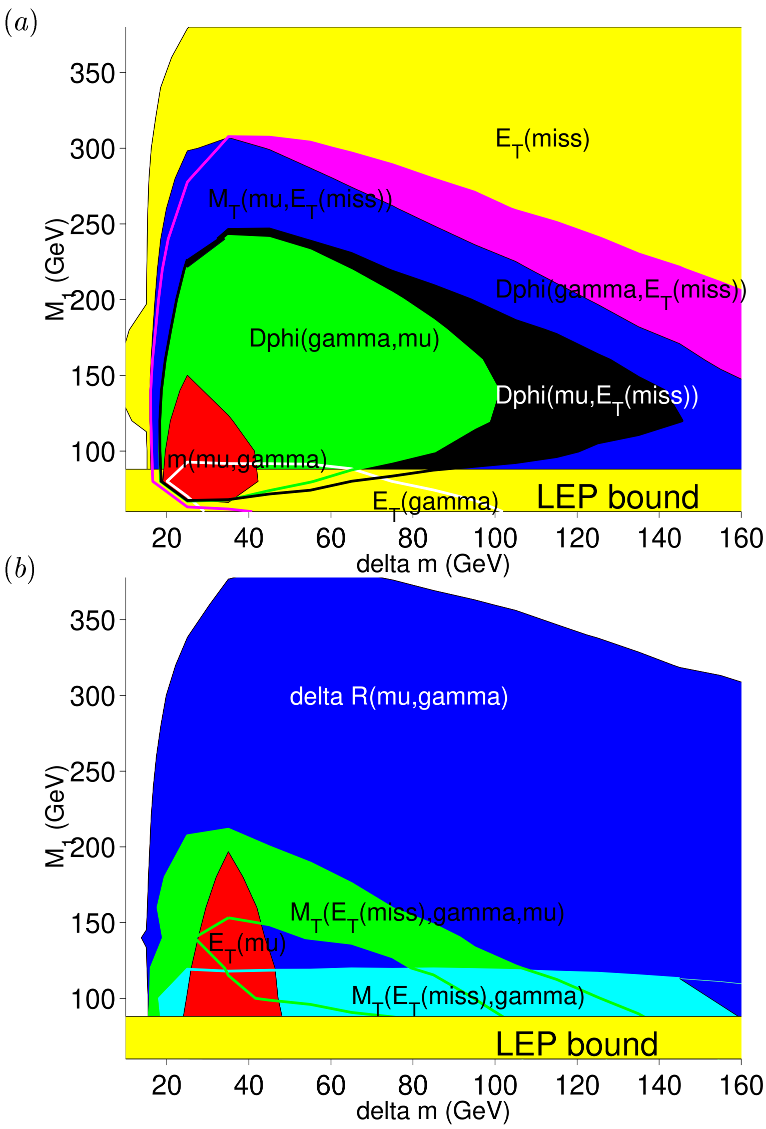

Figure 5: Separate good fit regions for each kinematical distribution. The horizontal region at the bottom of the plot displays the LEP bound from neutralino pair production where the neutralinos decay to photons and $\not{E}_T$ [16]. The horizontal axis is $\Delta m = m_{\tilde{l}-M_1}$. The kinematical variables are (a) $\not{E}_T$ (yellow), $\Delta\phi_{\gamma\not{E}_T}$ (magenta), $M_T(\mu\not{E}_T)$ (blue), $\Delta\phi_{\mu\not{E}_T}$ (black), $\Delta\phi_{\gamma\mu}$ (green), $m_{\mu\gamma}$ (red), $E_T(\gamma)$ (white line) and (b) $E_T(\mu)$ (red), $M_T(\not{E}_T, \gamma, \mu)$ (green), $M_T(\not{E}_T, \gamma)$ (cyan) and $\Delta R_{\mu\gamma}$ (blue).

physics background coming from γZ production, where $Z \to \nu\bar{\nu}$. We emphasise that measuring this interesting channel would provide an independent check on our model. In an R-parity conserving channel, a bound on the gravitino mass of $m_{\tilde{G}} > 2.7 \times 10^{-5}$ eV [18] comes from the non-observation of signal $\gamma\not{E}_T$ in D0 data [19]. They place a bound of roughly 10 signal events for minimum E_T's of 25 GeV at the 95% C.L. for a luminosity of 13 pb^{-1}. This would correspond to an upper bound of around 66 if we scale up to 86 pb^{-1}, as used here. The D0 bound is therefore not restrictive.[3] The predicted rate anyway depends heavily upon the values of the unfitted parameters (see conclusions).

[3] Also note that our cuts are completely different to those in the D0 analysis.

JHEP04(2002)002

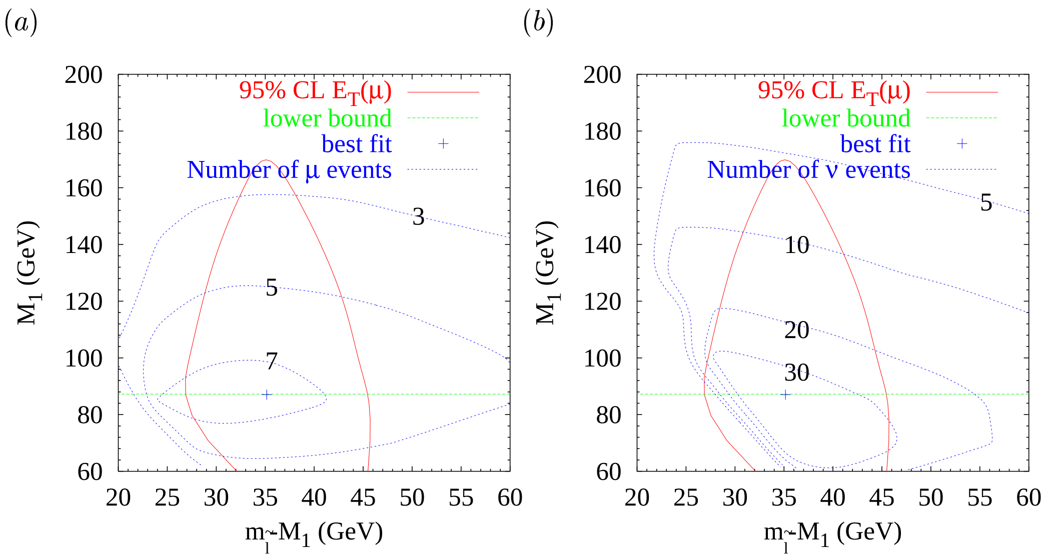

Figure 6: Expected number of (a) $\mu\gamma\not{E}_T$ and (b) $\gamma\not{E}_T$ signal events in Run I data. The dashed blue curves show (labeled) contours of number of expected events, the dotted green line shows the lower bound coming from LEP2 and the red curve shows the region of good fit $E_T(\mu)$ in the for $\mu\gamma\not{E}_T$ events.

In figure 7 we show the range of relevant masses and branching ratios over the best-fit region. As figure 7a indicates, $0.95 \leq BR(\tilde{\mu} \to \mu\chi_1^0) < 0.99$ in the best-fit region, thus other decay modes of resonant smuon production ought to be suppressed. Similarly, $0.91 \leq BR(\chi_1^0 \to \tilde{G}\gamma) < 0.98$ thus the competing $\not{R}_P$ (lepton and 2 jets) and $e^+e^-\tilde{G}$ decay modes of the resulting neutralino are also suppressed to unobservable levels at Run I. These branching ratios are dependent upon λ'_{211} and $m_{\tilde{G}}$. The range of viable right-handed smuon mass is $130 < m_{\tilde{\mu}_R} < 210\,\text{GeV}$, as shown in figure 7$c$. The lightest neutralino mass is approximately equal to M_1 and varies up to 170 GeV in the best-fit region, as shown in figure 7d.

The approximate level of other processes can be roughly estimated by calculating the expected numbers of pairs of sparticles at Run I. Neutralino production is predicted to be at an unobservable level, but the light sleptons have a non-negligible number of expected pairs produced at Run I. Using 86.34 pb of luminosity, we display the expected number of selectron, selectron-sneutrino and sneutrino pairs produced at Run I in figure 8. No experimental cuts at all have been applied to these events, so detected numbers of these events might be expected to be a factor of 5-10 less than the numbers that are displayed in the figure. We can see from figure 8a that in the 95% C.L. region that fits the $E_T(\mu)$ distribution, there are between about 0.1 and 1 selectron pairs expected, depending upon the actual value of the parameters Δm and M_1. The dominant decays of the selectrons is $\tilde{e} \to e\chi_1^0$, again followed by $\tilde{\chi}_1^0 \to \gamma\tilde{G}$. Thus the selectron pairs provide the correct signature to describe the $ee\gamma\gamma\not{E}_T$ event recorded by CDF at run I. When detector efficiencies taken into account, the expected number of $ee\gamma\gamma\not{E}_T$ events, while being less than one, are nevertheless still much higher than the expected Standard Model background. Selectron pair production is predicted to be at the same level as smuon pair

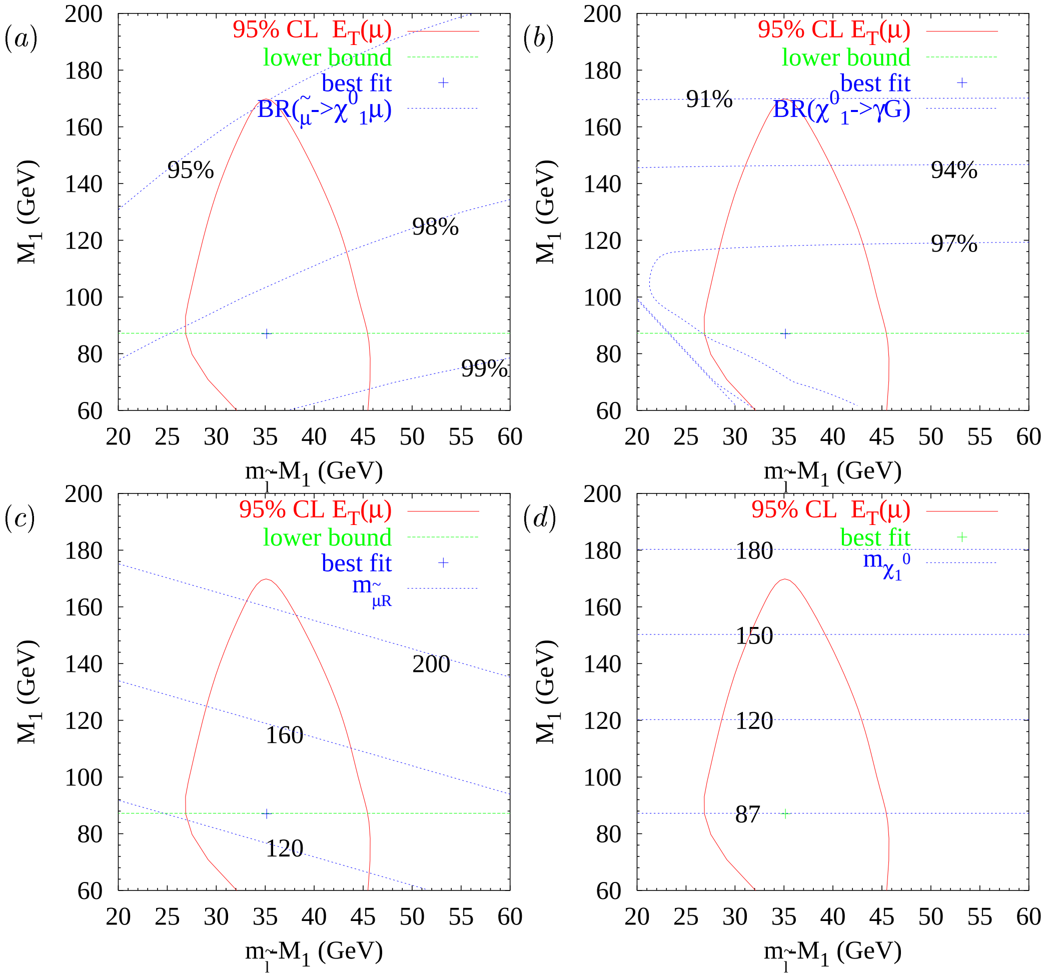

Figure 7: Relevant masses and branching ratios in the best-fit region. The dashed blue lines show (labeled) contours of (a) $BR(\tilde{\mu} \to \mu\chi_1^0)$, (b) $BR(\chi_1^0 \to \tilde{G}\gamma)$, (c) $m_{\tilde{\mu}_R}$ (GeV), (d) $m_{\chi_1^0}$ (GeV), the dotted green line shows the lower bound coming from LEP2 and the red curve shows the region of good fit $E_T(\mu)$ in the for $\mu\gamma\not{E}_T$ events.

production, since they have approximately equal masses and they are produced via gauge interactions. However, the muon detection efficiency is somewhat lower than for electrons, so the expected number of *detected* $\mu\mu\gamma\gamma\not{E}_T$ events from smuon pair production is smaller. It is also possible to produce sneutrinos, and selectron-sneutrino pairs (with final state $e\gamma\gamma\not{E}_T$) are predicted to be at the 0.1-2 event level before cuts. In figure 8*c*, we see that sneutrino pair production is predicted to be at the level of 0.1 to 2 events. This final state will manifest itself as $\not{E}_T\gamma\gamma$.

7. Predictions for Run II

At Run II of the Tevatron, assuming $2\,\text{fb}^{-1}$ of luminosity, our model can be ruled out or verified by again looking for an excess in the $\mu\gamma\not{E}_T$ channel, with much higher statistics. For example, assuming the same cuts and detector efficiencies as in our Run I analysis, we

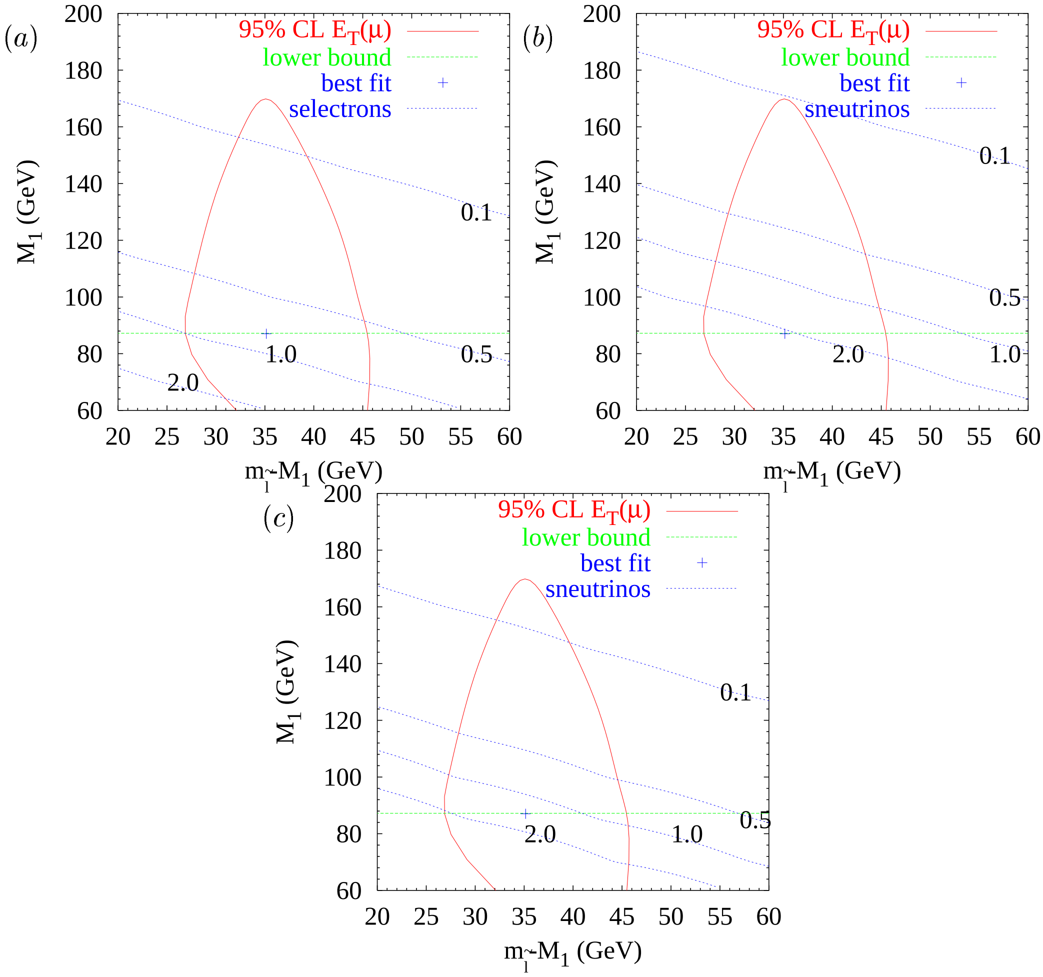

Figure 8: Number of (a) selectron, (b) selectron-sneutrino and (c) sneutrino pairs produced at run I of the Tevatron. The dashed blue lines show the expected number of events, the dotted green line shows the lower bound coming from LEP2 and the red curve shows the region of good fit $E_T(\mu)$ in the for $\mu\gamma\not{E}_T$ events.

expect 193 signal events at Run II for our best-fit point because the cross-section increases to 0.096 pb for detected events. This estimate will be subject to change once the relevant cuts and detector efficiencies for Run II are known. We also expect an excess of 740 events in the $\not{E}_T\gamma$ channel from resonant sneutrino production at the best-fit point. We calculate the number of events in the $\not{E}_T\mu\gamma$ and $\not{E}_T\gamma$ channel and display them in figure 9, assuming $2\,\mathrm{fb}^{-1}$ of collected luminosity (assuming the same efficiencies and cuts as used in Run I). We see that at least 70 events in the $\not{E}_T\mu\gamma$ channel are expected and at least 150 in the $\not{E}_T\gamma$ channel. This will be sufficient to measure parameters much more accurately, or rule the model out completely.

If a $\mu\gamma\not{E}_T$ signal is seen at Run II, the kinematic distributions will determine the viable parameter space more accurately than Run I data. Sparticle pair production may also be viable, and can provide constraints upon the parameter space. For this reason, we show the expected number of slepton pairs produced in figure 10. Figure 10a shows that between

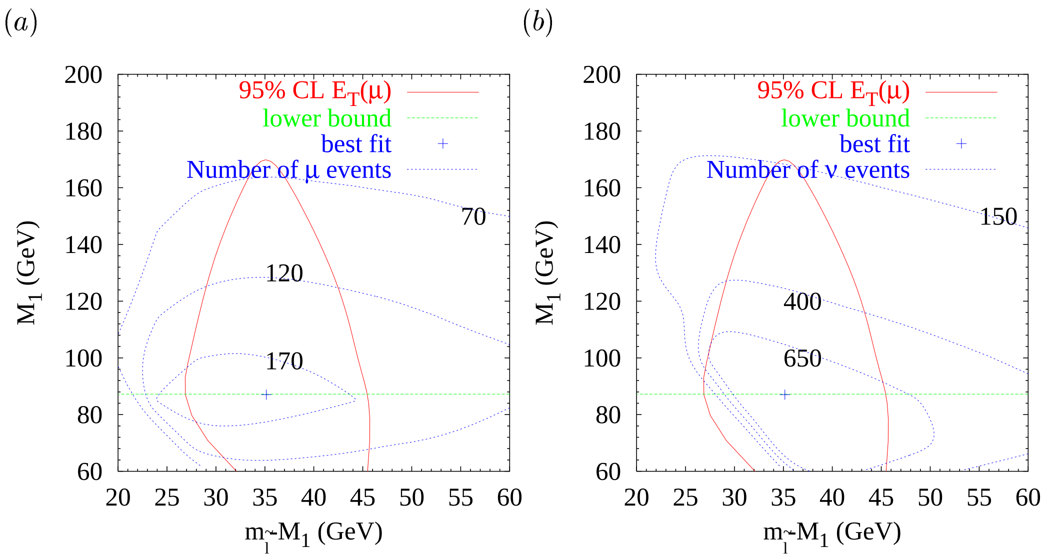

Figure 9: Expected number of (a) $\mu\gamma\not{E}_T$ and (b) $\gamma\not{E}_T$ signal events in Run II data. The dashed blue curves show (labeled) contours of number of expected events, the dotted green line shows the lower bound coming from LEP2 and the red curve shows the region of good fit $E_T(\mu)$ in the for $\mu\gamma\not{E}_T$ events.

2 and 30 selectron (and smuon) pairs are expected, between 3 and 50 sneutrino-selectron and sneutrino-smuon pairs (figure 10b), and between 2 and 40 sneutrino pairs (figure 10c). Once efficiencies and cuts are taken into account, this adds up to at most a handful of events in each channel. Nevertheless, this would provide independent confirmation for our scenario and Standard Model background rates would be still extremely low.

8. Conclusions

We have demonstrated that R-parity violating supersymmetry with a light gravitino can explain an anomalously high measured cross-section for the $\mu\gamma\not{E}_T$ channel. It also explains features observed in the kinematic variables of the signal events. We have used this information to constrain the slepton and neutralino mass parameters in the model. Whereas we could not perform a combined fit to all the different kinematic distributions, if $M_1 \approx 90$ and $\Delta m_{\tilde{l}} \approx 30\,\text{GeV}$, all of the distributions are fit well. Ideally a combined fit to all kinematical variables would be performed for our model and a measure of the fit probability calculated (along with that of the Standard Model). Such a fit would require simulation of the backgrounds as well as knowledge of the multi-dimensional distributions of variables rather than the one-dimensional projections available to us. We have seen qualitatively that the $ee\gamma\gamma\not{E}_T$ event observed in Run I is fit much better by our model than by the Standard Model.

We chose representative parameters $m_{\tilde{G}} = 10^{-3}\,\text{eV}$, $\lambda'_{211} = 0.01$ and $\tan\beta = 10$. Varying the first two parameters does not change the kinematics of the event, merely the branching ratios of the decays. Thus the total number of signal events in the relevant channel changes, but the kinematic shapes in the signal events remain the same. A higher

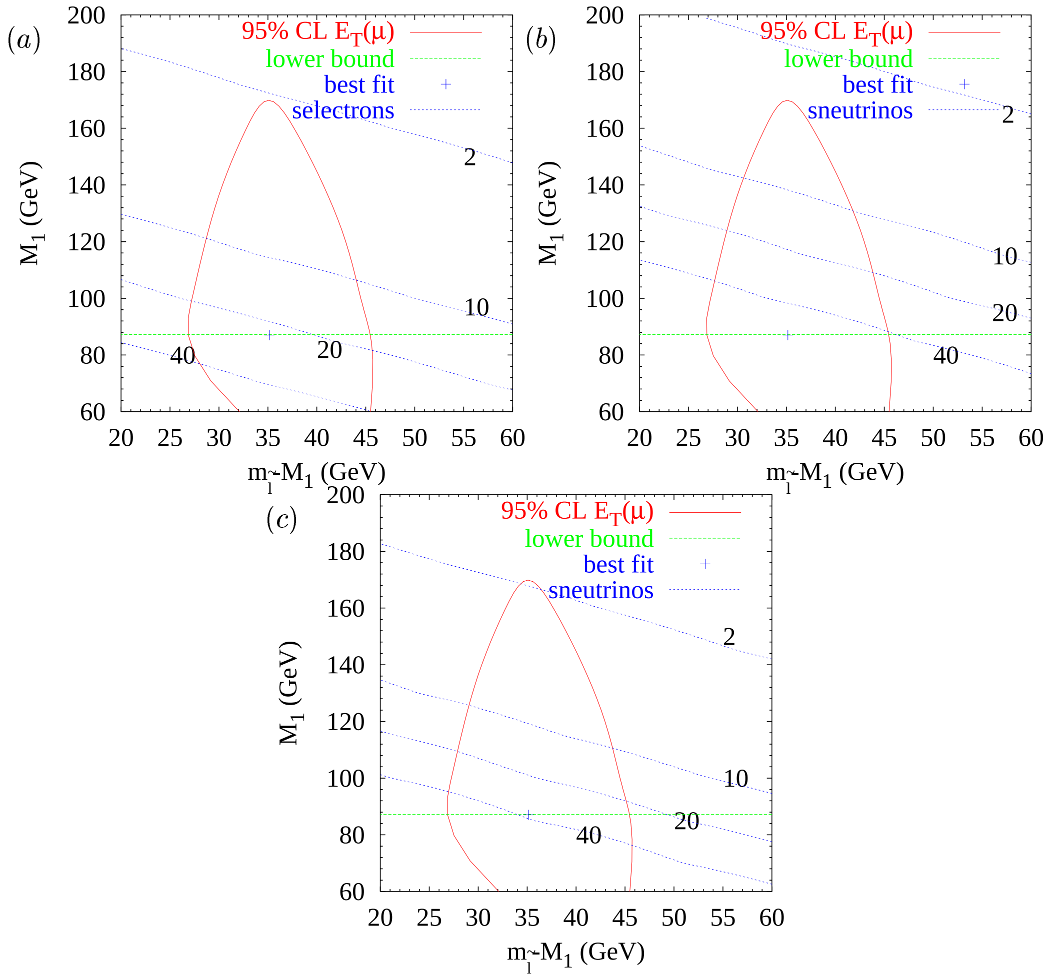

Figure 10: Expected number of sparticle pairs produced at run II of the Tevatron for $2\,\mathrm{fb}^{-1}$ luminosity. The dashed blue lines show the expected number of events for (a) selectron (b) selectron-sneutrino and (c) sneutrino pair production, the dotted green line shows the lower bound coming from LEP2 and the red curve shows the region of good fit for $\mu\gamma\not\!\!E_T$ events.

value of $m_{\tilde{G}}$ decreases the number of neutralinos decaying to a photon and a gravitino, but this can be compensated for by increasing λ'_{211} to increase the production cross-section. However, at some value of λ'_{211}, R-parity violating decays will dominate over the gravitino decays of the neutralino. We also note that changing $\tan\beta$ has the effect of changing the relationship between $m_{\tilde{l}}$ and the slepton masses, as eq. (5.3) shows. Thus, different values of $\tan\beta$ could potentially prefer different regions of Δm.

Higher values of λ'_{211} can also be accommodated by increasing both the mass of the sleptons and the mass of the neutralino to decrease the hard production cross-section. These points are illustrated in turn in table 4, where the parameters are all varied in such a way as to produce a number of events comparable to the best fit value of 7.8. Point 1 illustrates that a higher value for $m_{\tilde{G}}$, which gives lower branching ratios of $\chi_1^0 \to \gamma\tilde{G}$, can be compensated by an increase in λ'_{211}, raising the resonant smuon production cross-section. The kinematic fits still look favourable: point 1 fits the data better than the

Standard Model to $\Delta\sigma = 1.7 - 3.3$ depending upon the variable. However, it does seem difficult to raise $m_{\tilde{G}}$ further because the required increase in λ'_{211} then gives dominant decay modes to be R-parity violating, decreasing the number of signal events $N_{\not{E}_T\mu\gamma}$. Points 2 and 3 illustrate the insensitivity to values of $\tan\beta$. We note in point 4 that a heavy neutralino of 200 GeV also can provide enough events by raising λ'_{211}, but that the $E_T(\gamma)$ distribution is predicted to be too hard compared with the data. Also, the signal bump in $m_{\mu\gamma}$ goes to higher energies, disagreeing somewhat with the data. The other distributions seem to fit the data quite well however. Point 4 also shows that the predicted number of $\gamma\not{E}_T$ events does vary with λ'_{211} and $m_{\tilde{G}}$, and so our prediction for the numbers of these events is parameter dependent.

Run II will provide a definitive test of our scenario, by again looking in the $\mu\gamma\not{E}_T$ and $\not{E}_T\gamma$ channels. Other final states with small SM backgrounds are expected at the few-event level. For example, observation of $ee\gamma\gamma\not{E}_T$, $\mu\mu\gamma\gamma\not{E}_T$, $\mu\gamma\gamma\not{E}_T$ and $e\gamma\gamma\not{E}_T$ would provide independent confirmation of our scenario. We note, however, that towards the higher values of M_1 expected, less than one event in each of the pair production channels is likely once detector effects and cuts are taken into account.

Quantity	1	2	3	4
λ'_{211}	0.02	0.01	0.01	0.03
$m_{\tilde{G}}$ (eV)	0.01	10^{-3}	10^{-3}	10^{-3}
$\tan\beta$	10	20	5	10
Δm	35	40	35	35
M_1	87	87	87	200
$N_{\not{E}_T\mu\gamma}$	8.0	6.7	7.9	10.7
$N_{\not{E}_T\gamma}$	42	34	34	14
$\Delta\sigma(E_T(\mu))$	3.3	3.1	3.3	3.3
$\Delta\sigma(E_T(\gamma))$	1.8	1.9	1.9	-1.1
$\Delta\sigma(\not{E}_T)$	2.2	2.4	2.4	1.0
$\Delta\sigma(m_{\mu\gamma})$	2.6	2.3	2.6	-1.5
$\Delta\sigma(M_T(\not{E}_T\mu))$	2.1	2.5	2.3	1.9
$\Delta\sigma(M_T(\not{E}_T\gamma))$	2.8	3.0	2.9	0.6
$\Delta\sigma(M_T(\not{E}_T\gamma\mu))$	1.7	1.6	2.0	1.0
$\Delta\sigma(\Delta\phi_{\not{E}_T\gamma})$	2.0	2.2	2.1	2.1
$\Delta\sigma(\Delta\phi_{\mu\gamma})$	2.7	2.7	2.8	2.6
$\Delta\sigma(\Delta\phi_{\not{E}_T\mu})$	2.8	2.7	2.8	3.1
$\Delta\sigma(H_T)$	1.8	2.1	2.1	1.4
$\Delta\sigma(\Delta R_{\mu\gamma})$	2.3	2.3	2.4	2.7

Table 4: Examples of 4 different parameter points, showing the parameters, the number of predicted events ($N_{\not{E}_T\mu\gamma}, N_{\not{E}_T\gamma}$) and the number of σ that the point fits the data *better* than the Standard Model.

Acknowledgments

We would like to warmly thank H. Frisch and D. Toback for their gracious help and advice regarding the data. We would like to thank D. Hutchcroft for discussions concerning LEP data and A. Barr, G. Blair and J. Holt for discussions on the statistics. We also acknowledge discussions with G. Altarelli, J. Ellis and M. Mangano.

References

[1] B.C. Allanach, A. Dedes and H.K. Dreiner, *Bounds on R-parity violating couplings at the weak scale and at the GUT scale*, *Phys. Rev.* **D 60** (1999) 075014 [hep-ph/9906209]; H. Dreiner, in *Perspectives on supersymmetry*, G.L. Kane ed., World Scientific 1998; G. Bhattacharyya, *A brief review of R-parity-violating couplings*, presented at *Workshop on physics beyond the standard model*, Tegernsee, Germany, 8–14 June 1997 hep-ph/9709395.

JHEP04(2002)002

[2] For some of the earlier references, see F. Zwirner, *Observable $\Delta B = 2$ transitions without nucleon decay in a minimal supersymmetric extension of the standard model*, *Phys. Lett.* **B 132** (1983) 103;
L.J. Hall and M. Suzuki, *Explicit R parity breaking in supersymmetric models*, *Nucl. Phys.* **B 231** (1984) 419;
J.R. Ellis, G. Gelmini, C. Jarlskog, G.G. Ross and J.W.F. Valle, *Phenomenology of supersymmetry with broken R parity*, *Phys. Lett.* **B 150** (1985) 142;
S. Dawson, *R-parity breaking in supersymmetric theories*, *Nucl. Phys.* **B 261** (1985) 297;
R. Barbieri and A. Masiero, *Supersymmetric models with low-energy baryon number violation*, *Nucl. Phys.* **B 267** (1986) 679.

[3] G.F. Giudice and R. Rattazzi, *Theories with gauge-mediated supersymmetry breaking*, *Phys. Rept.* **322** (1999) 419 [hep-ph/9801271].

[4] S. Borgani, A. Masiero and M. Yamaguchi, *Light gravitinos as mixed dark matter*, *Phys. Lett.* **B 386** (1996) 189 [hep-ph/9605222].

[5] P. Fayet, *Mixing between gravitational and weak interactions through the massive gravitino*, *Phys. Lett.* **B 70** (1977) 461; *Lower limit on the mass of a light gravitino from e^+e^- annihilation experiments*, *Phys. Lett.* **B 175** (1986) 471.

[6] CDF collaboration, D. Acosta et al., *Search for new physics in photon lepton events in proton antiproton collisions at $\sqrt{s} = 1.8$ TeV*, hep-ex/0110015.

[7] B.C. Allanach, S. Lola and K. Sridhar, *Explaining anomalous CDF $\mu\gamma$ missing-E_T events with supersymmetry*, hep-ph/0111014.

[8] S. Dimopoulos, R. Esmailzadeh, L.J. Hall and G.D. Starkman, *Cross-sections for lepton and baryon number violating processes from supersymmetry at $p\bar{p}$ colliders*, *Phys. Rev.* **D 41** (1990) 2099;
J. Kalinowski, R. Rückl, H. Spiesberger and P.M. Zerwas, *R-parity violating SUSY signals in lepton pair production at the Tevatron*, *Phys. Lett.* **B 414** (1997) 297 [hep-ph/9708272];
J.L. Hewett and T.G. Rizzo, *Resonant slepton production at hadron colliders in R-parity violating models*, hep-ph/9809525;
B. Allanach et al., *Searching for R-parity violation at run-II of the Tevatron*, hep-ph/9906224;
H. Dreiner, P. Richardson and M.H. Seymour, *Resonant slepton production in hadron hadron collisions*, *Phys. Rev.* **D 63** (2001) 055008 [hep-ph/0007228];
H. Dreiner, P. Richardson and M. Seymour, *Parton-shower simulations of R-parity violating supersymmetric models*, *J. High Energy Phys.* **04** (2000) 008 [hep-ph/9912407]; *Resonant slepton production at the LHC*, hep-ph/0001224;
G. Moreau, M. Chemtob, F. Deliot, C. Royon and E. Perez, *Phys. Lett.* **B 475** (2000) 184;
G. Moreau, E. Perez and G. Polesello, *Resonant sneutrino production in supersymmetry with R-parity violation at the LHC*, *Nucl. Phys.* **B 604** (2001) 3 [hep-ph/0003012].

[9] S. Ambrosanio, G.L. Kane, G.D. Kribs, S.P. Martin and S. Mrenna, *Supersymmetric analysis and predictions based on the CDF $ee\gamma\gamma+$ missing e_t event*, *Phys. Rev. Lett.* **76** (1996) 3498 [hep-ph/9602239];
G.L. Kane and S. Mrenna, *Do about half the top quarks at FNAL come from gluino decays?*, *Phys. Rev. Lett.* **77** (1996) 3502 [hep-ph/9605351];
S. Ambrosanio, G.L. Kane, G.D. Kribs, S.P. Martin and S. Mrenna, *Low energy supersymmetry with a neutralino LSP and the CDF $ee\gamma\gamma$ + missing E_T event*, *Phys. Rev.* **D 55** (1997) 1372 [hep-ph/9607414].

JHEP04(2002)002

[10] H. Baer, M. Brhlik, C.-h. Chen and X. Tata, *Signals for the minimal gauge-mediated supersymmetry breaking model at the fermilab tevatron collider*, *Phys. Rev.* **D 55** (1997) 4463 [hep-ph/9610358].

[11] CDF collaboration, F. Abe et al., *Searches for new physics in diphoton events in $p\bar{p}$ collisions at $\sqrt{s} = 1.8$ TeV*, *Phys. Rev.* **D 59** (1999) 092002 [hep-ex/9806034].

[12] V.D. Barger, G.F. Giudice and T. Han, *Some new aspects of supersymmetry R-parity violating interactions*, *Phys. Rev.* **D 40** (1989) 2987.

[13] CDF collaboration, F. Abe et al., *Search for new particles decaying to dijets at CDF*, *Phys. Rev.* **D 55** (1997) 5263 [hep-ex/9702004].

[14] F.E. Paige, S.D. Protopopescu, H. Baer and X. Tata, *ISAJET 7.40: a Monte Carlo event generator for pp, $\bar{p}p$ and e^+e^- reactions*, hep-ph/9810440.

[15] G. Corcella et al., *Herwig 6.3*; *Herwig 6: an event generator for hadron emission reactions with interfering gluons (including supersymmetric processes)*, *J. High Energy Phys.* **01** (2001) 010 [hep-ph/0011363];
Herwig 6.3 release note, hep-ph/0107071;
Herwig: a Monte Carlo event generator for simulating hadron emission reactions with interfering gluons. Version 5.1 - April 1991, *Comput. Phys. Commun.* **67** (1992) 465.

[16] Particle Data Group, *Review of particle physics Eur. Phys. J.* **C 15** (2000) 1.

[17] D.E. Hutchcroft, *Searches for extra dimensions, gauge mediated SUSY and exotics at LEP*, hep-ex/0111085.

[18] A. Brignole, F. Feruglio, M.L. Mangano and F. Zwirner, *Signals of a superlight gravitino at hadron colliders when the other superparticles are heavy*, *Nucl. Phys.* **B 526** (1998) 136 [hep-ph/9801329].

[19] D0 collaboration, B. Abbott et al., *$Z\gamma$ production in $p\bar{p}$ collisions at $\sqrt{s} = 1.8$ TeV and limits on anomalous $ZZ\gamma$ and $Z\gamma\gamma$ couplings*, *Phys. Rev.* **D 57** (1998) 3817 [hep-ex/9710031].

JHEP04(2002)002